PCCP

Accepted Manuscript

ROYAL SOCIETY OF CHEMISTRY

www.rsc.org/pccp

ARTICLE www.rsc.org/[journal] | [journal name]

Nanometer-sized dynamic entities in an aqueous system

E. Mamontov*[a], P. Zolnierczuk[b], and M. Ohl[c]

Receipt/Acceptance Data **[DO NOT ALTER/DELETE THIS TEXT]**
Publication data **[DO NOT ALTER/DELETE THIS TEXT]**
DOI: 10.1039/b000000x [DO NOT ALTER/DELETE THIS TEXT]

Using neutron spin-echo and backscattering spectroscopy, we have found that at low temperatures water molecules in an aqueous solution engage in center-of-mass dynamics that are different from both the main structural relaxations and the well-known localized motions in the transient cages of the nearest neighbor molecules. While the latter localized motions are known to take place on the picosecond time scale and Angstrom length scale, the slower motions that we have observed are found on the nanosecond time scale and nanometer length scale. They are associated with the slow secondary relaxations, or excess wing dynamics, in glass-forming liquids. Our approach, therefore, can be applied to probe the characteristic length scale of the dynamic entities associated with slow dynamics in glass-forming liquids, which presently cannot be studied by other experimental techniques.

Introduction

Water is a very peculiar glass-forming liquid, characterized by the inaccessible "no man's land" region,[1] between the homogeneous ice nucleation temperature of *ca*. 231 K on cooling down and glassy water crystallization temperature of 150 K on warming up. Besides the main structural α-relaxation, studies of ambient and supercooled water reveal the picosecond time scale, Angstrom length scale, center-of-mass microscopic dynamics inside the transient cage made of the nearest neighbor molecules.[2] This dynamics, often referred to as β-fast, is arguably a common feature of liquids, whether glass-forming or not,[3] and is described in detail by the mode-coupling theory (MCT).[4-6]

Glass-forming liquids are also known to exhibit, at temperatures below $ca.1.2T_g$, much slower (but still faster than the α-relaxation) secondary relaxation dynamics, visible either as a distinct β-slow process, or the so-called excess wing near the main relaxation. Possible existence of such slow dynamics in water is an intriguing idea, with important implications for water-protein dynamic coupling and protein dynamic transition.[7-10] Evidence for such dynamics comes from a series of recent experiments on aqueous solutions of lithium chloride,[11-14] which, uniquely among aqueous solutions, are very similar in their dynamic properties to pure water,[15,16] yet allow measurements down to *ca*. 200 K in the thermodynamically stable liquid state without freezing.[17] In the current work we demonstrate that the characteristic length of the slow dynamic process in aqueous systems is about a nanometer, which is about 6 times larger than the characteristic length associated with the β-fast dynamics in the cage of the nearest neighbors. Similar to the Angstrom-sized transient nearest-neighbor cages that form and dissipate on the picosecond time scale below a certain temperature (when the β-fast process becomes separated from the main structural α-relaxation[18]), the nanometer-sized dynamic entities form and dissipate on the nanosecond and longer timescale, also below a certain temperature, when the β-slow or excess wing dynamics become separated from the main structural α-relaxation. The proposed data analysis approach, made possible by neutron scattering signal sensitivity to the scattering momentum transfer, *Q*, should be applied in the future to conventional glass-forming liquids to elucidate the spatial characteristics of the dynamic entities associated with the slow relaxations or excess wing dynamics. While other present-day experimental techniques cannot be used for such studies because of the lack of *Q*-resolution capabilities (dielectric spectroscopy, NMR), insufficient energy resolution (inelastic x-ray scattering), or unsuitable length scale (dynamic light scattering), x-ray photon correlation spectroscopy (XPCS) may have a future potential to yield similar information on glass-forming liquids.

Experiment

As in the earlier studies,[11-14] the sample, 7.6 m LiCl aqueous solution (molar composition of $(H_2O)_{0.88}(LiCl)_{0.12}$, or $(H_2O)_{7.3}(LiCl)$) was prepared using deoinized distilled water and anhydrous, ultra-dry lithium chloride powder (99.995 % purity) available commercially from Alfa Aesar. We used the neutron spin-echo (NSE) spectrometer[19,20] and the backscattering spectrometer BASIS[21] at the Spallation Neutron Source, Oak Ridge National Laboratory (ORNL). BASIS was operated in the standard regime, with 3.4 μeV energy resolution (full-width at half-maximum, *Q*-averaged value) and the dynamic range of ±100 μeV selected for the

[a] *Neutron Sciences Directorate, Oak Ridge National Laboratory, Oak Ridge, Tennessee, 37831-6473, USA. Fax: 1-865-574-6080; Tel: 1-865-771-1387; E-mail: mamontove@ornl.gov*
[b] *Juelich Center for Neutron Science , Outstation at the Spallation Neutron Source, Oak Ridge National Laboratory, Oak Ridge, Tennessee, 37831-6473, USA. Fax: 1-865-574-6080; Tel: 1-865-241-0092; E-mail: zolnierczukp@ornl.gov*
[c] *Juelich Center for Neutron Science , Outstation at the Spallation Neutron Source, Oak Ridge National Laboratory, Oak Ridge, Tennessee, 37831-6473, USA. Fax: 1-865-574-6080; Tel: 1-865-574-8426; E-mail: m.ohl@fz-juelich.de*

data analysis. The sample was loaded into an annular cylindrical sample holder with an outer diameter of 29.0 mm and an inner diameter of 28.9 mm, resulting in a sample thickness of 0.05 mm. For the NSE experiment, the sample was loaded into a flat-plate aluminum container, which was 5 cm tall, 3 cm wide, and 0.25 mm thick. The NSE measurements at two scattering angles, yielding the average Q values of 0.53 and 0.65 Å^{-1}, were carried out with an incident wavelengths band between 5 Å and 8 Å. Due to the rather low signal, the NSE intensity has been integrated over the wavelength band from approximately 5.3 Å to 7.7 Å. This wavelength spread translates into the maximum spread in Fourier times of $\Delta\tau/\tau$ = 0.44 and the maximum spread in Q values of (0.53 ± 0.07) Å^{-1} and (0.65 ± 0.09) Å^{-1}. A maximum resolution of about 22 ns was achieved. Corrections were performed using the separately collected resolution data. A standard TiZr sample was used to collect the resolution data set for the NSE experiment, whereas in the BASIS experiment the resolution was collected from the sample itself cooled down to 5 K. The use of the coherently scattering TiZr for the resolution measurement resulted in the negative spin-echo amplitudes for the predominantly incoherently scattering sample; this was addressed and corrected in the course of data reduction. The measured (from the empty cell) background contribution to the $I(Q,t)$ data points was found to be quite small, ranging from ca. 6 % to ca. 0.5 %, depending on the Fourier time, which was much smaller compared to the statistical error. The NSE measurements were carried out at 201 K, as in the previous experiment,[14] whereas the BASIS measurements were performed at 290, 280, 270, 260, 250, 240, 230, 220, 210, and 200 K, followed by the resolution measurement. It was essential to collect the NSE data at a low temperature of 201 K because a clear separation between the dynamic components of interest within the dynamic range of the NSE was required (provided that the main relaxation still remained within the spectrometer resolution in the investigated Q range). At temperatures lower than 201 K, freezing of the sample could not be ruled out. As a measure of goodness of data fits we used the parameter $\chi^2 = \Sigma(I_{\text{experiment}} - I_{\text{model}})^2/(N_{\text{observations}} - N_{\text{parameters}})$, or reduced χ^2, which accounts for the difference in the number of fit parameters.

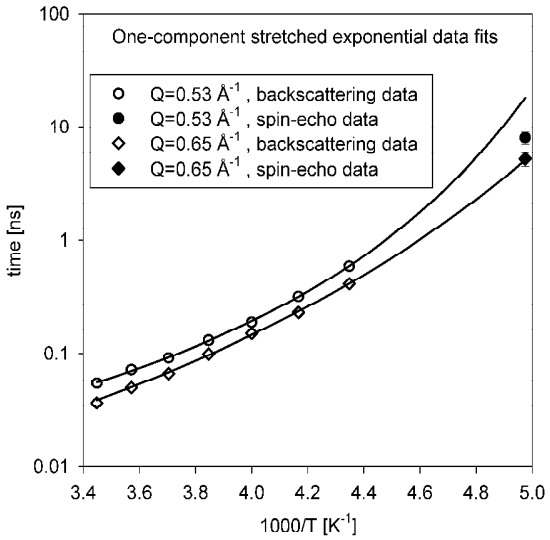

Fig. 1 Average relaxation times for water molecules in $(H_2O)_{0.88}(LiCl)_{0.12}$ obtained from one-component stretched exponential data fits (the fit parameters used to compute the backscattering relaxation times are given in Table 1). Note that only the backscattering data for T ≥ 230 K, but not the spin-echo relaxation times were used for the VFT fits (solid lines).

Results and discussion

The central idea of the 201 K data analysis is the notion that NSE can probe both the α- and β-slow relaxations (but not the much faster β-fast relaxation), and, therefore, the time-space NSE signal can be described by a two-component decay:[14]

$$I(Q,t) = (1 - p(Q))\exp\left[-\left(\frac{t}{\tau_*}\right)^{\beta}\right] + p(Q)\exp\left[-\left(\frac{t}{\tau_\alpha}\right)^{\beta}\right] \quad (1)$$

where both the α- and β-slow relaxations contribute to the initial decay time, $1/\tau_* = [(1/\tau_{\beta\text{-}slow})^{\beta} + (1/\tau_\alpha)^{\beta}]^{1/\beta}$, and $p(Q)$ is the elastic incoherent structure factor (EISF) for the β-slow relaxation motions in the transient "confinement". The latter parameter is of ultimate interest to us since its Q-dependence yields the characteristic size of the dynamic entities associated with the slow secondary relaxations. Importantly, Eq. (1) has been derived for the single-particle dynamics, and is valid for hydrogenated samples that scatter neutrons predominantly incoherently. Thus, the simple form of Eq. (1) that allows intuitive interpretation is associated with a serious challenge as far as NSE measurements are concerned, given the loss of statistics in spin-echo data collected from incoherently scattering samples. Exacerbating the problem is the need to measure one Q value at a time. Indeed, it took us a total of two weeks of NSE beam time to collect the data at Q = 0.53 Å^{-1} and Q = 0.65 Å^{-1} for one single temperature of 201 K. Backscattering spectrometry, on the other hand, readily measures the single-particle dynamics from the hydrogenated, incoherently scattering samples, over a broad Q range simultaneously, but lacks the energy resolution to probe the α-relaxation at low temperatures. Therefore, the effective strategy is to use backscattering at T ≥ 230 K, where the α- and β-slow relaxations are merged, and the characteristic time of this merged relaxation process is comfortably within the resolution of the backscattering technique, fit the backscattering data with a single stretched exponential component, and then extrapolate the results down to T = 201 K to obtain input for the NSE data analysis. Both the backscattering and spin-echo experiments probe the single-particle dynamics of water molecules in the solution due to the dominant (incoherent) neutron scattering cross-section of hydrogen.[22]

The data presented in Figure 1 was obtained using this approach. The main purpose of Figure 1 is to illustrate and explain the fact that a two-component fit of NSE data was possible and even needed at Q = 0.53 Å^{-1}, but not possible at Q = 0.65 Å^{-1}. At Q = 0.65 Å^{-1}, the Vogel-Fulcher-Tammann (VFT) fit, $\tau = \tau_0\ exp(DT_0/(T-T_0))$, of the backscattering relaxation times yielded $\tau_0 = (0.63 \pm 0.49)\times10^{-3}$ ns, $D = (5.4 \pm 2.1)$, $T_0 = (126.0 \pm 16.0)$ K, which extrapolates to 5.1 ns for T = 201 K. This relaxation time predicted from the backscattering data is in excellent agreement with the independently fitted spin-echo value of (5.2 ± 0.7) ns, obtained from the 201 K NSE data stretched exponential fit with $\tau_0 = (4.8 \pm 0.3)$ ns and $\beta = (0.87 \pm 0.06)$. Furthermore, this single-component stretched exponential fit of the NSE data (Figure 2) with agreement factor of of $\chi^2 = 2.954$ could not be improved when we attempted to use a two Debye-like component fit (that is, $\beta = 1$ in Eq. (1)). In fact, the spectral weight of the second component invariably converged to zero, which is not surprising in view of the fact that a single-component relaxation time already matches the extrapolation of the high-temperature backscattering data (Figure 1), leaving no room for another component. Thus, a single stretched exponential component decay is the appropriate model for the NSE data at Q = 0.65 Å^{-1}, and there is no room for a second component in the 201 K data fit, nor any need for such a component to achieve agreement between the high-temperature backscattering data and the NSE data.

The situation is drastically different for Q = 0.53 Å^{-1}. The VFT fit of the backscattering relaxation times yielded $\tau_0 = (3.0 \pm 0.7)\times10^{-3}$ ns, $D = (2.5 \pm 0.4)$, $T_0 = (156.1 \pm 4.8)$ K, which extrapolates to 18.2 ns for T = 201 K. This relaxation time predicted from the backscattering data far exceeds the fitted spin-echo value of (8.0 ± 1.0) ns, obtained from the 201 K NSE data stretched exponential fit with $\tau_0 = (7.5 \pm 0.4)$ ns and $\beta = (0.88 \pm 0.06)$. This strongly indicates that a single stretched exponential component fit of the NSE data may not be adequate at Q = 0.53 Å^{-1}. Indeed, with 6 degrees of freedom, the 95 % confidence level limit for the reduced χ^2 is 2.099. The single stretched exponential fit yields $\chi^2 = 2.282$, which allows us to reject the hypothesis that a single stretched exponential function describes our data at the 95 % confidence level. On the other hand, the two Debye-like component fit ($\beta = 1$, with a fixed $\tau_\alpha = 18.2$ ns in Eq. (1)), yields $\chi^2 = 1.483$, which is as good as the random noise allows. The resulting fit parameter is $\tau_* = (5.5 \pm 0.9)$ ns, or $\tau_{\beta\text{-}slow} = (7.9 \pm 2.2)$ ns.

We want to emphasize that, while the improved fit quality of the $I(Q,t)$ might provide circumstantial evidence for the presence of two relaxation components, the compelling need to introduce the second component at Q = 0.53 Å^{-1} comes from the mismatch between the one-component NSE data fit and the extrapolation of the backscattering data. This mismatch is observed at Q = 0.53 Å^{-1}, but not at Q = 0.65 Å^{-1}. Furthemore, this mismatch for the 0.53 Å^{-1} data is fully analogous to our previous observations[14] made for the same sample and temperature at Q = 0.45 Å^{-1}. At that Q value, a single stretched exponential fit of the NSE data yielded the average relaxation time of (14.9 ± 1.3) ns, far shorter than the 27.4 ns relaxation time predicted by the VFT fit of the backscattering data, which necessitated a two-component fit of the NSE data. The main argument in favor of (at Q = 0.45 Å^{-1} and 0.53 Å^{-1}) or against (at Q = 0.65 Å^{-1}) a two-component fit is the comparison with the extrapolation of the high-temperature backscattering data, as long as the quality of the two-component fit is at least comparable with that of the single stretched exponential fit. The actually improved fit quality attained with the former compared to the latter model lends still more credence to the two-component description of the relaxation pattern.

Fgiure 3 shows the relaxation times from all of the NSE and backscattering data fits at the three Q values. For the NSE data sets collected at lower Q and temperature, two-component fits (1) yeild somewhat better agreement compared to the standard single stretched-exponential data fits, and, more importantly, (2) are needed to reconcile the NSE data with the extrapolated high-temperature backscattering data. The faster of the two components derived from the two-component fits of the NSE data are in good agreement with the backscattering results. At the same time, for the Q = 0.65 Å^{-1} data set, good agreement is observed between the NSE and extrapolation of the high-temperature backscattering relaxation times when both NSE and backscattering relaxation times are obtained from single-component fits, despite deviation of the low-temperature backscattering data from the VFT fit. These observations suggest that quantitative interpretation of the backscattering relaxation times at low temperatures is not always certain; depending on the temperature, Q value, and energy resolution, they might not represent the main structural relaxation, which could remain unresolved. For quantitative interpretation of low-temperature relaxation times, NSE should be used.

The spectral weight parameter $p(Q)$ in Eq. (1), which has a value of (0.45 ± 0.03) at Q = 0.45 Å^{-1} (Ref. 14) and (0.26 ± 0.08) at Q = 0.53 Å^{-1} as found in this work, is the EISF for the faster of the two dynamic processes in the transient confinement, which eventually dissipates through the slower of the two dynamic processes.[14] In the case of the β-fast dynamics in water,[2] the EISF for the β-fast process could be fit with a "diffusion in a sphere" model,[22] EISF(Q) = $[3j_1(Qa)/(Qa)]^2$, where j_1 is the first order spherical Bessel function, to yield the a = 0.73 Å radius for the transient cage of the nearest neighbors in which the β-fast process takes place. The β-fast dynamics is not merely rotational, but involves the center of mass motions of water molecules, leading to the Q-dependent β-fast relaxation times and the corresponding Q-dependent QENS broadening.[2] We have found that the same holds true for the presently investigated β-slow dynamics at 201 K. The relaxation times are $\tau_{\beta\text{-}slow}$ = (12.6 ± 3.4) ns at Q = 0.45 Å^{-1} (Ref. 14) and $\tau_{\beta\text{-}slow}$ = (7.9 ± 2.2) ns at Q = 0.53 Å^{-1} as found in the current work. Thus, the β-slow dynamics is not purely rotational and must involve the center-of-mass motions, in agreement with the earlier suggestions regarding the slow relaxations in water.[23] A fit of the $p(Q)$ with EISF(Q) = $[3j_1(Qa)/(Qa)]^2$ yields a radius of a = 4.36 Å^{-1} for the β-slow dynamics, as shown in Figure 4 inset.

A rather steep decay of the EISF due to the relatively large value of the radius of the transient confinement may explain why the two-component dynamics becomes undetectable in

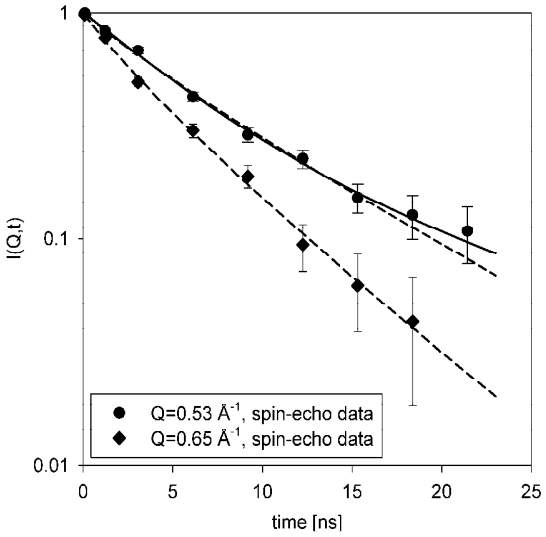

Fig. 2 Fits of the NSE $I(Q,t)$ at T =201 K with a single-component stretched exponential decay (dashed lines) and a two-component Debye-like decay (solid line).

our experiment already at Q = 0.65 Å^{-1}. Still, a rather sizable value of ca. 0.18 would be expected at this Q from EISF(Q) = $[3j_1(Qa)/(Qa)]^2$. It is possible that the simple two-component relaxation pattern described by Eq. (1) no longer holds at this and higher Q values. A possibility that the main structural relaxation is invariably coupled with a more localized process at higher Q values, thus rendering Eq. (1) invalid, is suggested by examination of the backscattering relaxation times. The critical temperature of the VFT fit, T_0 = (148 ± 16) K at Q = 0.45 Å^{-1} (Ref. 14) and T_0 = (156 ± 5) K at Q = 0.53 Å^{-1} (this work), indicates, as expected, the divergence of the main structural relaxation times on approaching the glass transition temperature of the system of *ca.* 140 K.[19] On the other hand, T_0 = (126 ± 16) K at Q = 0.65 Å^{-1}, possibly indicating the contribution to the scattering signal of the more localized dynamics that does not cease below T_g. This effect becomes even more pronounced at still higher Q values of 0.7 Å^{-1} and 0.9 Å^{-1}, where the backscattering data can be fitted by Arrhenius rather than VFT law,[11] which is incompatible with the presence of the main structural relaxation alone. Thus, the breakdown of the simple two-component relaxation pattern, which assumes decoupling between the separate relaxation processes as described by Eq. (1), is possible already at Q ≥ 0.65 Å^{-1}.

Table 1. The fit parameters for the single-component Fourier-transformed stretched exponential fits of the backscattering neutron data in the energy space. Also shown are the average relaxation times computed as $\langle\tau\rangle = (\tau/\beta)\Gamma(1/\beta)$, where Γ is the gamma-function, used to plot the data in Figures 1 and 3. The standard deviation values are shown in parentheses.

T, K	Q = 0.53 Å^{-1}			Q = 0.65 Å^{-1}		
	τ, ns	β	$\langle\tau\rangle$, ns	τ, ns	β	$\langle\tau\rangle$, ns
290	0.0477 (0.0011)	0.79 (0.02)	0.0546 (0.0024)	0.0264 (0.0014)	0.65 (0.02)	0.0362 (0.0030)
280	0.0654 (0.0010)	0.84 (0.01)	0.0721 (0.0023)	0.0439 (0.0011)	0.80 (0.02)	0.0499 (0.0023)
270	0.0842 (0.0010)	0.85 (0.01)	0.0916 (0.0025)	0.0563 (0.0012)	0.76 (0.01)	0.0663 (0.0026)
260	0.1193 (0.0012)	0.85 (0.01)	0.1303 (0.0030)	0.0851 (0.0012)	0.77 (0.01)	0.0989 (0.0029)
250	0.1703 (0.0018)	0.84 (0.01)	0.1874 (0.0044)	0.1304 (0.0014)	0.79 (0.01)	0.1497 (0.0036)
240	0.2838 (0.0030)	0.81 (0.01)	0.3177 (0.0074)	0.2038 (0.0020)	0.81 (0.01)	0.2282 (0.0049)
230	0.5058 (0.0080)	0.77 (0.01)	0.5916 (0.0181)	0.3580 (0.0041)	0.78 (0.01)	0.4128 (0.0100)
220	0.7650 (0.0189)	0.73 (0.01)	0.9350 (0.0422)	0.5512 (0.0093)	0.76 (0.01)	0.6493 (0.0217)
210	1.4490 (0.1409)	0.63 (0.02)	2.0657 (0.2831)	1.0780 (0.0522)	0.68 (0.02)	1.4102 (0.1080)
200	5.2880 (1.237)	0.57 (0.04)	8.6036 (2.5913)	2.5980 (0.5516)	0.61 (0.03)	3.8275 (1.0316)

An important question is whether the observed transient nanometer-sized entities associated with the slow center-of-mass dynamics is a general property of aqueous systems. Because of the same onset temperature[25,26] in the case of lithium chloride aqueous solutions and pure water in confinement,[16] the β-slow dynamics that we analyse in the current work could be a property of water not specific to lithium chloride solutions. It is known that adding a salt provides the means to prevent water freezing without resorting to nano-confinement[16] while retaining the parameters characteristic of pure water such as the same T_g[15] and largely intact water-water hydrogen bonding.[27,28] Besides, the ion hydration complexes in aqueous solutions of lithium chloride are unstable on the nano-second time scale[29,30] and thus unable to contribute to the β-slow dynamics that we observe. Therefore, our results suggest that nanometer-sized (in diameter) entities of dynamic nature may play the same role of transient confinement for the β-slow dynamics in water as the Angstrom-sized dynamic entities made by the transient nearest neighbors play for the β-fast relaxation in water. In the intermediate temperature range shown in Figure 4, the β-slow and α-relaxations are merged because the nanometer-sized dynamic entities are not sustained even in the transient state. Similarly, the cages of the nearest neighbors are not sustained at very high temperatures even in the transient state, thus leading to the eventual merging of the β-fast and α-processes.[3]

For water and liquids in general, the interpretation of the Angstrom-sized dynamic entities as nearest neighbors' cages is intuitive, whereas the interpretation of the nanometer-sized dynamic entities is not. We can hypothesize that the split of the slow secondary relaxation from the α-processes below *ca.* 230 K may be related to the dynamic heterogeneity phenomenon in water.[31,32] Even though the four-point correlation function, $\chi_4(Q,t)$, which describes the dynamic heterogeneity,[33] is not measurable in a neutron scattering experiment, the closely related experimentally accessible dynamic susceptibility can indicate dynamic heterogeneities even in the incoherent scattering signal from H_2O.[31,32]

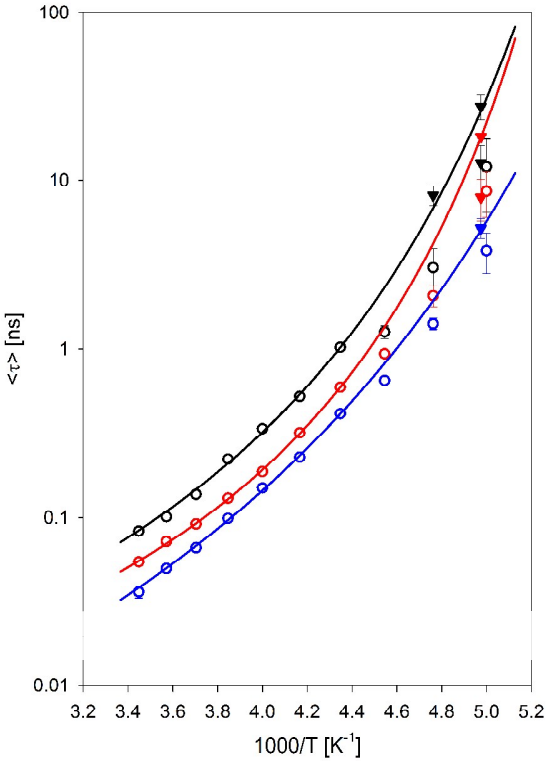

Fig. 3 Backscattering (open circles) and NSE (filled down triangles) relaxation times. Black: $Q = 0.45$ Å^{-1} (Ref. 14). Red: $Q = 0.53$ Å^{-1} (current work). Blue: $Q = 0.65$ Å^{-1} (current work). The relaxation times are obtained from single stretched-exponential fits, except for NSE data at $T = 201$ K, $Q = 0.45$ Å^{-1} and 0.53 Å^{-1}, which require two-component fits. The solid lines are VFT fits of the backscattering relaxation times at $T \geq 230$ K.

Likewise, the nanometer-sized dynamic entities manifest themselves in our experiment on a hydrogenated system, which probes single-particle, not collective relaxation dynamics. Furthermore, the dynamics of these entities are associated with center-of-mass, not purely rotational motions. A simple Eq. (1), derived for single-particle dynamics, describes such center-of-mass motions as the internal dynamics of the transient domains that eventually dissipate through the main structural relaxations. Eq. (1) also provides the means to extract the characteristic domain size. In this scenario, the intra-domain dynamics give rise to the β-slow (or excess wing) relaxations, whereas the α-relaxation annihilates the domains.

The presence of the β-slow (or excess wing) relaxations is common in glass-forming liquids at sufficiently low temperatures. Thus, a combination of neutron incoherent backscattering and spin-echo measurements, exactly as outlined in the current work, should be universally applicable to probing the spatial extent of the slow relaxations in liquids. Such a feat, at present unattainable by other experimental techniques, is ultimately made possible by the Q-dependence of the inelastic neutron scattering signal over the probed length scale of about an Angstrom to several nanometers.

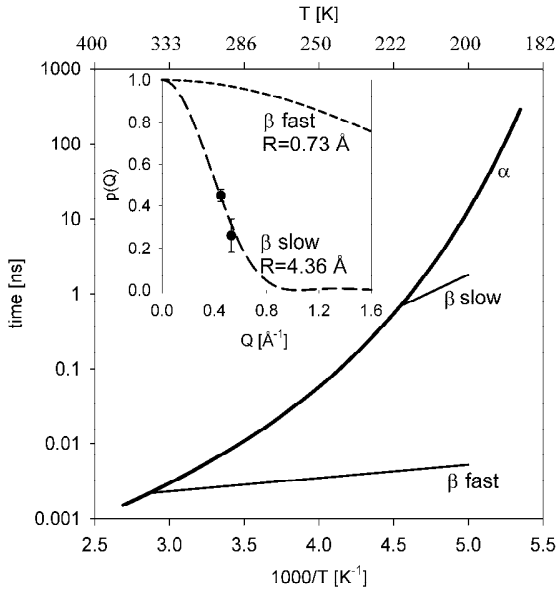

Fig. 4 A schematic diagram of the microscopic relaxation dynamics of water and aqueous systems if the structural arrest below *ca*. 228 K could be avoided (adopted from Ref. 24, temperatures and relaxation times are approximate). Inset: fits of the elastic incoherent structure factor with a "diffusion in a sphere" model,[22] EISF(Q) = $[3j_1(Qa)/(Qa)]^2$, yielding the transient confinement radius of 0.73 Å (from Ref. 2) and 4.36 Å (this work) for the β-fast and β-slow dynamics, respectively.

Conclusions

At sufficiently low temperatures, water molecules in an aqueous solution of lithium chloride engage in the slow center-of-mass dynamics that are different from both the main structural relaxations and the localized motions in the transient cages of the nearest neighbor molecules. Using inelastic neutron scattering, we have probed the Q-dependence of this slow secondary relaxation, or excess wing, dynamics of water molecules in order to elucidate the spatial characteristics of these motions. These slow dynamics are associated with the transient nanometer-sized entities, just as the fast dynamics inside the nearest-neighbor cages are known to be associated with the Angstrom-sized transient entities. Similar to the Angstrom-sized transient nearest-neighbor cages that form and dissipate on the picosecond time scale below a certain temperature, when the fast dynamics become separated from the main structural relaxation, the nanometer-sized dynamic entities form and dissipate on the nanosecond and longer timescale, also below a certain temperature, when the slow dynamics become separated from the main structural relaxation. Our approach to the experiment and data analysis can be applied to probe the characteristic length scale of the dynamic entities associated with slow dynamics in glass-forming liquids, which presently cannot be studied by other experimental techniques.

Acknowledgement

The neutron scattering studies were conducted with support from the Scientific User Facilities Division, Office of Basic Energy Sciences, U.S. DOE. Oak Ridge National Laboratory is managed by UT-Battelle, LLC, for U.S. DOE under Contract No. DE-AC05-00OR22725.

Notes and references

1 O. Mishima and H. E. Stanley, *Nature*, 1998, **396**, 329.
2 J. Qvist, H. Schober, and B. Halle, *J. Chem. Phys.*, 2011, **134**, 144508.
3 E. Mamontov, *J. Phys. Chem. B*, 2013, **117**, 9501.
4 W. Götze and L. Sjögren, *Rep. Prog. Phys.*, 1992, **55**, 241.
5 W. Götze, *J. Phys.: Condens. Matter*, 1999, **11**, A1.
6 W. Götze, Complex dynamics of glass forming liquids. A mode-coupling theory, Oxford University Press, Oxford, U. K. (1999).
7 S.-H. Chen, L. Liu, E. Fratini, P. Baglioni, A. Faraone, and E. Mamontov, *Proc. Nat. Acad. Sci.*, 2006, **103**, 9012.
8 S. Khodadadi, S. Pawlus, and A. P. Sokolov, *J. Phys. Chem. B*, 2008, **112**, 14273.
9 W. Doster, S. Busch, A. M. Gaspar, M.-S. Appavou, J. Wuttke, and H. Scheer, *Phys. Rev. Lett.*, 2010, **104**, 098101.
10 S. Magazu, F. Migliardo, and A. Benedetto, *J. Phys. Chem. B*, 2011, **115**, 7736.
11 E. Mamontov, *J. Phys. Chem. B*, 2009, **113**, 14073.
12 E. Mamontov, A. Faraone, E. W. Hagaman, K. S. Han, and E. Fratini, *J. Phys. Chem. B*, 2010, **114**, 16737.
13 M. Nakanishi, P. Griffin, E. Mamontov, and A. P. Sokolov, *J. Chem. Phys.*, 2012, **136**, 124512.
14 E. Mamontov and M. Ohl, *Phys. Chem. Chem. Phys.*, 2013, **15**, 10732.
15 C. A. Angell and E. J. Sare, *J. Chem. Phys.*, 1970, **52**, 1058.
16 E. Mamontov, D. R. Cole, S. Dai, M. D. Pawel, C. D. Liang, T. Jenkins, G. Gasparovic, and E. Kintzel, *Chem. Phys.*, 2008, **352**, 117.
17 A. Elarby-Aouizerat, J.-F. Jal, P. Chieux, J. M. Letoffe, P. Claudy, and J. Dupuy, *J. Non-Cryst. Solids*, 1988, **104**, 203.
18 D. Chandler and J. P. Garrahan, *Annu. Rev. Phys. Chem*, 2010, **61**, 191.
19 M. Ohl, M. Monkenbusch, D. Richter, C. Pappas, K. Lieutenant, Th. Krist, G. Zsigmond, and F. Mezei, *Physica B*, 2004, **350**, 147.
20 M. Ohl, M. Monkenbusch, N. Arend, T. Kozielewski, G. Vehres, C. Tiemann, M. Butzek, H. Soltner, U. Giesen, R. Achten, H. Stelzer, B. Lindenau, A. Budwig, H. Kleines, M. Drochner, P. Kaemmerling, M. Wagener, R. Moller, E. B. Iverson, M. Sharp, and D. Richter, *Nucl. Instrum. Methods A*, 2012, **696**, 85.
21 E. Mamontov and K. W. Herwig, *Rev. Sci. Inst.*, 2011, **82**, 085109.
22 M. Bée, Quasielastic Neutron Scattering, Hilger, Bristol (1988).
23 K. L. Ngai, S. Capaccioli, S. Ancherbak, and N. Shinyashiki, *Phil. Mag.*, 2011, **91**, 1809.
24 E. Mamontov and X. Chu, *Phys. Chem. Chem. Phys.*, 2012, **14**, 11573.
25 M. E. Gallina, L. Bove, C. Dreyfus, A. Polian, B. Bonello, R. Cucini, A. Taschin, R. Torre, and R. M. Pick, *J. Chem. Phys.*, 2009, **131**, 124504.
26 S. C. Santucci, L. Comez, F. Scarponi, G. Monaco, R. Verbeni, J.-F. Legrand, C. Masciovecchio, A. Gessini, and D. Fioretto, *J. Chem. Phys.*, 2009, **131**, 154507.
27 D. A. Turton, C. Corsaro, D. F. Martin, F. Mallamace, and K. Wynne, *Phys. Chem. Chem. Phys.*, 2012, **14**, 8067.
28 L. Le and V. Molinero, *J. Phys. Chem. A*, 2011, **115**, 5900.
29 N. A. Hewish, J. E. Enderby, and W. S. Howells, *J. Phys. C.: Solid State Phys.*, 1983, **16**, 1777.
30 P. S. Salmon, *J. Phys. C.: Solid State Phys.*, 1987, **20**, 1573.
31 Y. Zhang, M. Lagi, F. Ridi, E. Fratini, P. Baglioni, E. Mamontov, and S.-H. Chen, *J. Phys.: Condens. Matter*, 2008, **20**, 502101.
32 Y. Zhang, M. Lagi, E. Fratini, P. Baglioni, E. Mamontov, and S.-H. Chen, *Phys. Rev. E*, 2009, **79**, 040201.
33 L. Berthier, G. Brioli, J.-P. Bouchaud, L. Cipelletti, D. El Masri, D. L'Hote, F. Ladieu, and M. Pierno, *Science*, 2005, **310**, 1797.